

# Reversal of the detrimental effects of social isolation on ischemic cerebral injury and stroke-associated pneumonia by inhibiting small intestinal $\gamma\delta$ T-cell migration into the brain and lung

Bing Xie<sup>1,2,\*</sup>, Yujing Zhang<sup>1,2,\*</sup>, Mengqi Han<sup>1,2,\*</sup>,  
Mengyuan Wang<sup>1,2</sup>, Yuan Yu<sup>1,2</sup>, Xiaoyan Chen<sup>1,2</sup>,  
Yuming Wu<sup>1,2</sup>, Kenji Hashimoto<sup>3</sup>, Shiyong Yuan<sup>1,2</sup>,  
You Shang<sup>1,2</sup> and Jiancheng Zhang<sup>1,2</sup>

## Abstract

Social isolation (ISO) is associated with an increased risk and poor outcomes of ischemic stroke. However, the roles and mechanisms of ISO in stroke-associated pneumonia (SAP) remain unclear. Adult male mice were single- or pair-housed with an ovariectomized female mouse and then subjected to transient middle cerebral artery occlusion. Isolated mice were treated with the natriuretic peptide receptor A antagonist A71915 or anti-gamma-delta ( $\gamma\delta$ ) TCR monoclonal antibody, whereas pair-housed mice were treated with recombinant human atrial natriuretic peptide (rhANP). Subdiaphragmatic vagotomy (SDV) was performed 14 days before single- or pair-housed conditions. We found that ISO significantly worsened brain and lung injuries relative to pair housing, which was partially mediated by elevated interleukin (IL)-17A levels and the migration of small intestine-derived inflammatory  $\gamma\delta$  T-cells into the brain and lung. However, rhANP treatment or SDV could ameliorate ISO-exacerbated post-stroke brain and lung damage by reducing IL-17A levels and inhibiting the migration of inflammatory  $\gamma\delta$  T-cells into the brain and lung. Our results suggest that rhANP mitigated ISO-induced exacerbation of SAP and ischemic cerebral injury by inhibiting small intestine-derived  $\gamma\delta$  T-cell migration into the lung and brain, which could be mediated by the subdiaphragmatic vagus nerve.

## Keywords

Stroke-associated pneumonia, atrial natriuretic peptide, gamma-delta T cells, social isolation, subdiaphragmatic vagus nerve

Received 8 November 2022; Revised 9 March 2023; Accepted 16 March 2023

## Introduction

Globally, stroke is one of the leading causes of mortality and sustained disability, and it contributes to 10% of global deaths.<sup>1</sup> The major determinants of poor clinical outcome after stroke are a spectrum of medical

\*These authors contributed equally to this work.

### Corresponding authors:

Jiancheng Zhang, Union Hospital, Tongji Medical College, Huazhong University of Science and Technology, 1277 Jiefang Avenue, Wuhan, Hubei 430022, China.  
Email: zhjcheng1@126.com

You Shang, Union Hospital, Tongji Medical College, Huazhong University of Science and Technology, 1277 Jiefang Avenue, Wuhan, Hubei 430022, China.  
Email: you\_shanghust@163.com

Shiyong Yuan, Union Hospital, Tongji Medical College, Huazhong University of Science and Technology, 1277 Jiefang Avenue, Wuhan, Hubei 430022, China.  
Email: yuan\_shiyong@163.com

<sup>1</sup>Department of Critical Care Medicine, Union Hospital, Tongji Medical College, Huazhong University of Science and Technology, Wuhan, P.R. China

<sup>2</sup>Institute of Anesthesia and Critical Care Medicine, Union Hospital, Tongji Medical College, Huazhong University of Science and Technology, Wuhan, P.R. China

<sup>3</sup>Division of Clinical Neuroscience, Chiba University Center for Forensic Mental Health, Chiba, Japan

complications, among which stroke-associated pneumonia (SAP) is the most frequent and severe complication. SAP occurs most often within the first 7 days of stroke onset<sup>2</sup> and is reported to be associated with a 49% increase in 1-year mortality.<sup>3</sup> Accumulating clinical and experimental studies have recognized aberrant immune responses as a critical contributor to the development of SAP.<sup>4,5</sup> Despite sustained efforts to investigate preventive therapies for SAP, prophylactic antibiotics have failed to reduce the incidence of SAP.<sup>6,7</sup> Therefore, providing a clear understanding of the underlying mechanisms of SAP is critical for improving the efficacy of clinical treatments for patients at high risk of SAP.

Social isolation (ISO), characterized by reduced social contact and connections, has increasingly been recognized as a public health priority.<sup>8</sup> Emerging evidence has indicated a compelling association between ISO and an increased risk of stroke.<sup>9,10</sup> Social deprivation contributes to accelerated disease progression and impaired recovery from stroke,<sup>11–13</sup> which has been recapitulated by experimental models.<sup>14,15</sup> In contrast, social support potentially decreases the detrimental impacts of maladaptive psychological responses to stress and has been linked epidemiologically with improved functional recovery from stroke.<sup>15–17</sup> However, it remains elusive whether different housing conditions play a role in SAP.

Accumulating evidence has demonstrated that atrial natriuretic peptide (ANP), a cardiovascular hormone produced by the heart atria,<sup>18</sup> exerts protective effects in various diseases.<sup>19–24</sup> Plasma ANP levels are lower in depressive patients than in healthy individuals.<sup>25,26</sup> Furthermore, due to its ability to regulate fluid and electrolyte balance in order to reduce brain edema, ANP has been investigated in animal experiments for its neuroprotective role in brain injury. Exogenous administration of recombinant human ANP (rhANP) markedly reduced infarct volume and improved neurofunctional status in a preclinical study of stroke.<sup>27</sup> Clinical studies have also shown that ANP may exert beneficial effects in stroke,<sup>28</sup> partially by regulating cerebral flow.<sup>29</sup> Additionally, ANP has pleiotropic effects that drive the immune response, with powerful modulatory effects on many aspects of cellular and humoral immunity, including suppressing the synthesis and release of proinflammatory mediators,<sup>19,30</sup> enhancing the natural cytotoxicity of natural killer cells, and increasing macrophage phagocytosis.<sup>19</sup> ANP functions by binding to natriuretic peptide receptor A,<sup>24</sup> which is highly expressed in intestinal epithelial cells.<sup>31</sup> We previously reported that ANP is involved in post-stroke ISO-mediated depression;<sup>24</sup> however, the role of ANP in the impact of ISO on ischemic cerebral injury and SAP remains unclear.

The intestinal tract is the largest and most sophisticated immune organ of the entire body,<sup>32</sup> and the

extensive repertoire of intestinal immune cells and highly innervated nature of the gut mucosa make it a critical organ that affects the immune homeostasis of distant organs, such as the brain,<sup>21,33,34</sup> lung<sup>35–37</sup> and liver.<sup>38</sup> Evidence has shown that 50% of stroke survivors experience gastrointestinal complications,<sup>39</sup> which in turn exacerbate stroke outcomes through dysregulation of the gut microbiota and aberrant inflammatory responses.<sup>39,40</sup> Furthermore, the innate immune response plays a pivotal role in the development of stroke-induced pulmonary infections.<sup>41</sup> Gama-delta ( $\gamma\delta$ ) T cells are a subset of innate lymphocytes located mainly in the lamina propria of the small intestinal mucosa that act in a major histocompatibility complex-unrestricted manner. Although  $\gamma\delta$  T cells only account for a small part of the total T-cell pool, they are crucial in maintaining epithelial tissue integrity, repair, and host homeostasis, and in inhibiting pathogen infections.<sup>42</sup> However, there is evidence that abnormally activated  $\gamma\delta$  T cells function in the pathogenesis of inflammatory diseases.<sup>43</sup> In the proinflammatory environment caused by the destruction of the intestinal epithelial barrier and bacterial invasion, intestinal  $\gamma\delta$  T cells are transformed into an inflammatory phenotype that produces interleukin (IL)-17A and mediates inflammatory processes.<sup>44</sup> Mounting evidence has demonstrated that the blood–brain barrier is damaged in stroke progression, thus allowing the infiltration of activated CD4<sup>+</sup> and CD8<sup>+</sup> T cells, which are found to exacerbate neuroinflammation and restrain the recovery to ischemic stroke by secreting inflammatory cytokines.<sup>45–47</sup> Studies have shown that activated intestine-derived  $\gamma\delta$  T cells can also potentiate the progression of cerebral ischemic injury by migrating to the brain and influencing the local neuroinflammatory response through the secretion of IL-17A and IL-23.<sup>48,49</sup> However, the exact role of small intestinal  $\gamma\delta$  T cells in cerebral ischemic injury and SAP and the mechanisms behind migration have not yet been clarified.

We previously reported a critical role of the sub-diaphragmatic vagus nerve-mediated gut-brain axis in LPS-triggered endotoxemia and sepsis-induced cognitive disorder.<sup>21,34</sup> In this study, we investigated whether rhANP could attenuate ISO-induced exacerbation of SAP and ischemic cerebral injury by inhibiting sub-diaphragmatic vagus nerve-mediated migration of small intestine-derived  $\gamma\delta$  T cells into the lung and brain.

## Materials and methods

### Animals

Wild-type (WT) C57BL/6J mice (male, 23.0–25.0 g, 8–10 weeks) were purchased from Vital River

Laboratory Animal Technology Co Ltd., Beijing, China. Kaede-transgenic (Kaede-Tg) mice (B6.Cg-Gt (ROSA)26Sor<sup>tm1.1(CAG-kikGR)Kgw</sup>) were kindly provided by M. Tomura (Tokyo University). All animals were housed and maintained on a 12:12 light/dark schedule in ambient temperature and humidity-controlled specific pathogen-free conditions with free access to food and water. All experiments were approved by the committee of experimental animals of Tongji Medical College (Permission number: S2402) and complied with the National Institutes of Health Guide for the Care and Use of Laboratory Animals. All experiments were reported in compliance with the ARRIVE guidelines (Animal Research: Reporting *in Vivo* Experiments).

### **Transient Middle cerebral artery occlusion (MCAO) procedure**

Mice were subjected to MCAO, followed by reperfusion 1 hour later, as described in our previous studies.<sup>50–53</sup>

### **Photoconversion and cell migration analysis**

Kaede-Tg mice were used to monitor cellular migration. Kaede-Tg mice ubiquitously express the photoconvertible Kaede-Green fluorescent protein, which can switch into Kaede-Red upon photoactivation with near-UV light (350–410 nm). We employed the migration index to reflect the degree of migration of  $\gamma\delta$  T cells to other sites, which was calculated as Kaede Red<sup>+</sup> CD3<sup>+</sup>  $\gamma\delta$  TCR<sup>+</sup>/Kaede Green<sup>+</sup> CD3<sup>+</sup>  $\gamma\delta$  TCR<sup>+</sup>. Detailed information is provided in the supplemental material.

### **Experimental design and treatment**

The experiment was performed in three parts. Detailed information is provided in the supplemental material.

### **Behaviour tests**

Neurological deficit scores, open field test and cylinder test were assessed at 1 day and 3 days after MCAO. Detailed information is provided in the supplemental material.

### **Enzyme-linked immunosorbent assay (ELISA)**

Detailed information is provided in the supplemental material.

### **Lung wet/dry (W/D) weight ratio**

Lung edema was evaluated according to the wet/dry weight ratio of lung tissues. Detailed information is provided in the supplemental material.

### **2,3,5-Triphenyl-tetrazolium chloride (TTC) staining**

Following MCAO, the infarct volume was evaluated by TTC staining. Detailed information is provided in the supplemental material.

### **Myeloperoxidase (MPO) activity determination**

Detailed information is provided in the supplemental material.

### **Evans blue dye permeability assay**

Detailed information is provided in the supplemental material.

### **Total subdiaphragmatic vagotomy (SDV)**

Bilateral SDV or sham operation was performed 14 days prior to being randomly assigned to either single- or pair-housed conditions according to our previous studies.<sup>21,54,55</sup>

### **Hematoxylin-eosin (HE) staining**

Detailed information is provided in the supplemental material.

### **Bacterial counting**

Detailed information is provided in the supplemental material.

### **Flow cytometric analysis**

Detailed information is provided in the supplemental material.

### **16S rRNA analysis**

Detailed information is provided in the supplemental material.

### **Western blotting**

Detailed information is provided in the supplemental material.

### **Statistical analysis**

Data are expressed as the mean  $\pm$  standard deviation (SD). The normality of the datasets was established by the Kolmogorov–Smirnov test and the Shapiro–Wilk test. All datasets passed the normality test.

Multiple comparisons were performed by one-way ANOVA followed by *post hoc* Newman–Keuls multiple comparison tests. The comparisons of two values were evaluated by unpaired Student's *t* test. Correlation was analyzed by Pearson correlation.  $P < 0.05$  was considered statistically significant. Statistical analysis was performed using GraphPad Prism 8 software (GraphPad Software Inc., San Diego, CA, USA).

## Results

### *Effects of rhANP on ischemic brain injuries and associated pulmonary infections in isolated mice*

To examine whether pre-stroke housing manipulation influenced stroke outcomes, all mice were initially isolated or pair housed for two weeks prior to MCAO (Figure 1(a)). Significantly larger infarct volumes were observed in ISO mice at 24 and 72 hours post-reperfusion than in PH stroke mice (Figure 1(b) to (d)). To assess whether the neuroprotective role of PH was due to the increased level of ANP, we measured the serum levels of ANP in sham-operated and MCAO mice under different living conditions and found that stroke significantly reduced the serum ANP levels 24 and 72 hours post-reperfusion (Figure 1(e)). Moreover, PH significantly elevated circulating ANP concentrations in both sham-operated mice and MCAO mice 24 and 72 hours post-stroke (Figure 1(e)). We then investigated the effect of rhANP treatment on cerebral ischemic injury in stroke mice. We tried three levels of dose escalation of rhANP and found that the optimal dose of rhANP (1.0  $\mu\text{g/g}$ ) noticeably improved the brain infarct volume of isolated-housed mice 72 hours post-reperfusion, although this improvement did not reach statistical significance 24 hours post-reperfusion (Figure 1(b) to (d)). We chose to use the highest dose of rhANP in our subsequent experiments because this dose was associated with a significantly greater efficacy in improving cerebral ischemic injury. To validate the beneficial effect of rhANP, we used the ANP receptor antagonist A71915 in PH mice, and ANP markedly abrogated the improved effect of PH on infarct volumes (Figure 1(b) to (d)). The detrimental effect of ISO on ischemic brain injury was also reflected in higher neurological deficit scores in comparison with the PH group, and the functional outcomes of ISO stroke mice improved when treated with rhANP (Figure 1(f)). Measurements of regional cerebral blood flow (rCBF) by laser Doppler flowmetry established that there were no overt differences in rCBF among the three groups; thus, differences in stroke outcomes due to surgical factors were excluded (Supplemental Figure 1(a)). We further employed the open field test and the cylinder test to assess behavioral

changes post-stroke, and the results revealed significantly higher locomotor activities in PH mice and ISO mice injected with rhANP than in ISO mice 24 hours and 72 hours post-stroke (Figure 1(g) and (h)). In addition, there was significantly elevated MPO activity in ISO mice compared to PH mice 24 and 72 hours after MCAO, suggesting more severe inflammation in ISO stroke mice. Furthermore, rhANP treatment significantly reduced MPO activity in ISO stroke mice (Figure 1(i)). In addition, we detected spontaneous pneumonia in mice following MCAO. Of note, compared to PH mice, ISO mice exhibited worse outcomes in regard to bacterial load, MPO activity, lung wet/dry weight ratio and histological lung injury; all of which were attenuated by rhANP treatment (Figure 2(a) to (d)).

Furthermore, we found that the brain infarct volume was significantly positively correlated with pulmonary CFUs ( $r = 0.558$ ,  $P < 0.001$ ; Figure 2(e)) and MPO activity ( $r = 0.423$ ,  $P = 0.002$ ; Figure 2(f)) in all subjects from the six groups. Moreover, we also found a positive correlation between cerebral MPO activity and pulmonary MPO activity ( $r = 0.433$ ,  $P = 0.002$ ; Figure 2(h)), indicating that brain injury severity after acute ischemic stroke is directly related to the severity of SAP. In addition, pulmonary MPO activity was positively correlated with bacterial load in the lung ( $r = 0.442$ ,  $P = 0.001$ ; Figure 2(i)), suggesting that bacterial infection in the lung caused a strong inflammatory response. Overall, our results indicate that housing conditions prior to stroke are a strong determinant of short-term outcomes in post-stroke mice complicated with pneumonia and ANP serves as a key component in this process; furthermore, pair housing has a protective effect and isolated housing has a detrimental effect on both the brain and lungs.

### *Alteration of gut microbiota and $\gamma\delta$ T cells in rhANP-mediated stroke that was aggravated by ISO*

Next, we sought to elucidate the mechanisms of the varied effects of by housing conditions on SAP. Given the increased gut permeability that we observed in ISO stroke mice, we hypothesized that ISO may exacerbate SAP by disrupting the gut microbiota. However, our data indicated no significant differences in gut microbiota composition and relative abundance among mice subjected to isolated housing, paired housing and normal rearing (Supplemental Figure 2). Apart from this, rhANP and its antagonist A71915 did not cause any significant effects on gut microbiota (Supplemental Figure 2). Therefore, the 16S rRNA sequencing analysis negated our first conjecture that gut dysbiosis mediated the deleterious effects of ISO on SAP.



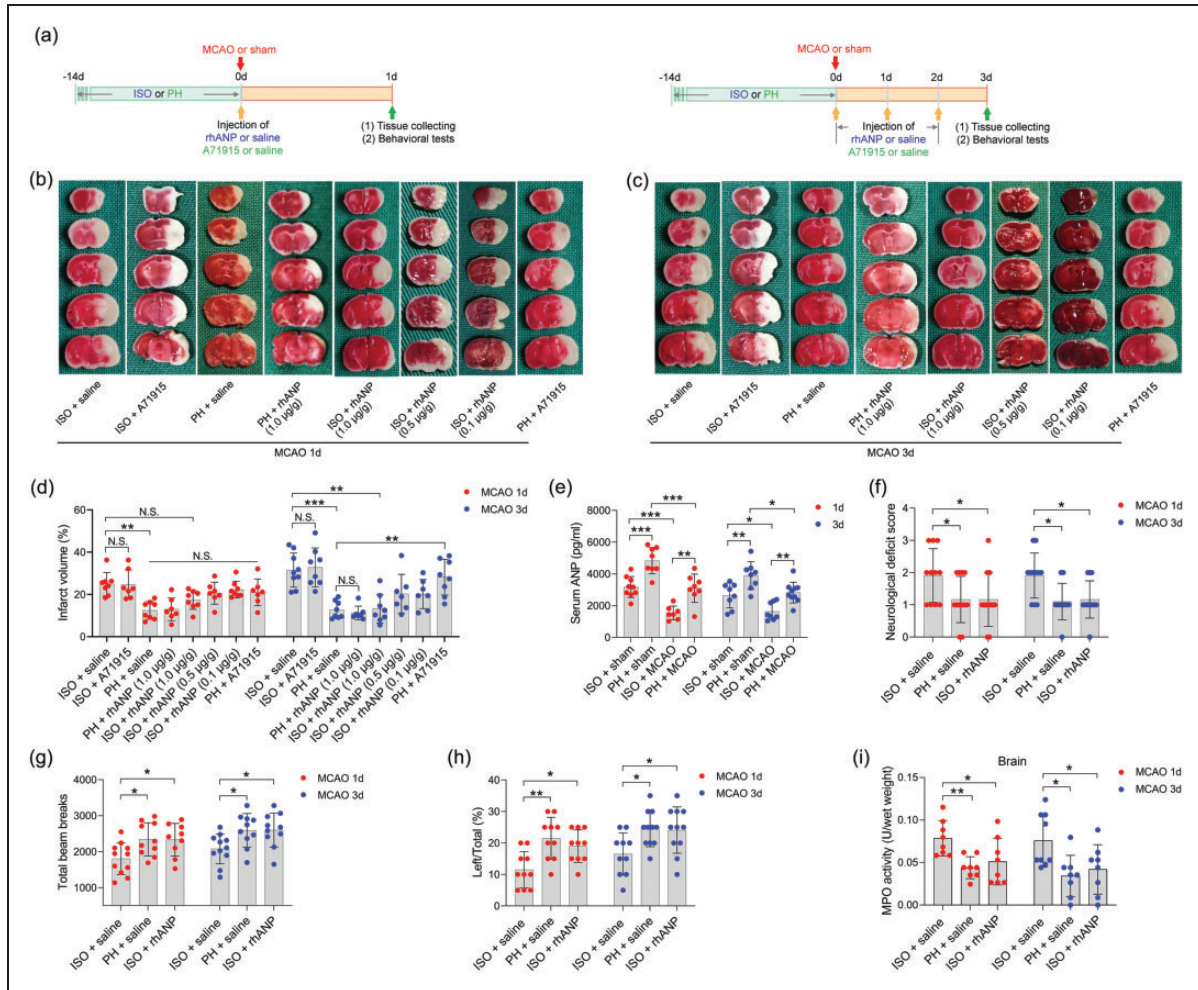


**Figure 1.** Pre-stroke ISO aggravated ischemic brain damage, which could be reversed by rhANP. (a) Treatment schedule. Mice were single- or pair-housed for 14 days before MCAO or sham operation. Recombinant human ANP (rhANP; 0.1 mg/kg, 0.5 mg/kg, 1.0  $\mu$ g/kg) or 0.9% saline was intravenously injected into mice on Day 1 after MCAO. Natriuretic peptide receptor A selective antagonist A71915 (0.5 mg/kg) or 0.9% saline was intraperitoneally injected into mice on Day 0 (right after MCAO surgery), Day 1 and Day 2 post-MCAO for mice tested on Day 3 after MCAO. Serum, brain and lung tissues were collected on Day 1 or Day 3 post-MCAO for analysis. Behavioral tests were conducted on Day 1 or Day 3 post-MCAO. (b, c) Diagram indicating the infarct area and peri-infarct area. (d) Infarct volumes were calculated as the percentage of infarct volume to whole brain. (e) Serum concentration of ANP. (f) Neurological deficit score. (g) Total beam breaks in the open field test represent spontaneous locomotor activity. (h) The use of the contralateral paw in the cylinder test was determined by the percentage of left/total and (i) Cerebral MPO activity. Data are presented as individual values plus means  $\pm$  SDs ( $n = 7-11$ /group). Comparisons were determined by one-way ANOVA followed by post hoc Newman–Keuls multiple comparison tests. N.S., not significant, \* $P < 0.05$ , \*\* $P < 0.01$ , \*\*\* $P < 0.001$ . ISO, isolated housing; MCAO, middle cerebral artery occlusion; PH, pair housing; rhANP, recombinant human atrial natriuretic peptide.

Previous studies have demonstrated the causal involvement of peripheral immune cells in ischemic brain injury and associated pneumonia.<sup>4</sup> Moreover, emerging evidence suggests that gut inflammatory responses play a key role in the pathophysiology of stroke.<sup>48,49</sup> Therefore, we identified  $\gamma\delta$  T cells, a critical lymphocyte population located at epithelial surfaces<sup>42</sup> mainly in the lamina propria of small intestine (SI-LP), and investigated them as a potential immunomodulator in the pathogenesis of ischemic stroke. We found a marked increase in the amount of  $\gamma\delta$  T cells in the

brain and lung of ISO mice compared to that of PH mice post stroke; however, rhANP administration completely reversed the increase in  $\gamma\delta$  T cells induced by ISO treatment (Figure 3(a) to (d)). Furthermore, similar changes were also observed in the blood (Figure 3(e) and (f)), although they did not reach statistical significance 24 hours post-reperfusion between mice subjected to ISO and PH. These results suggest that activation of  $\gamma\delta$  T cells may aggravate ischemic cerebral injury and associated pneumonia through migration to the injury sites. Considering that  $\gamma\delta$

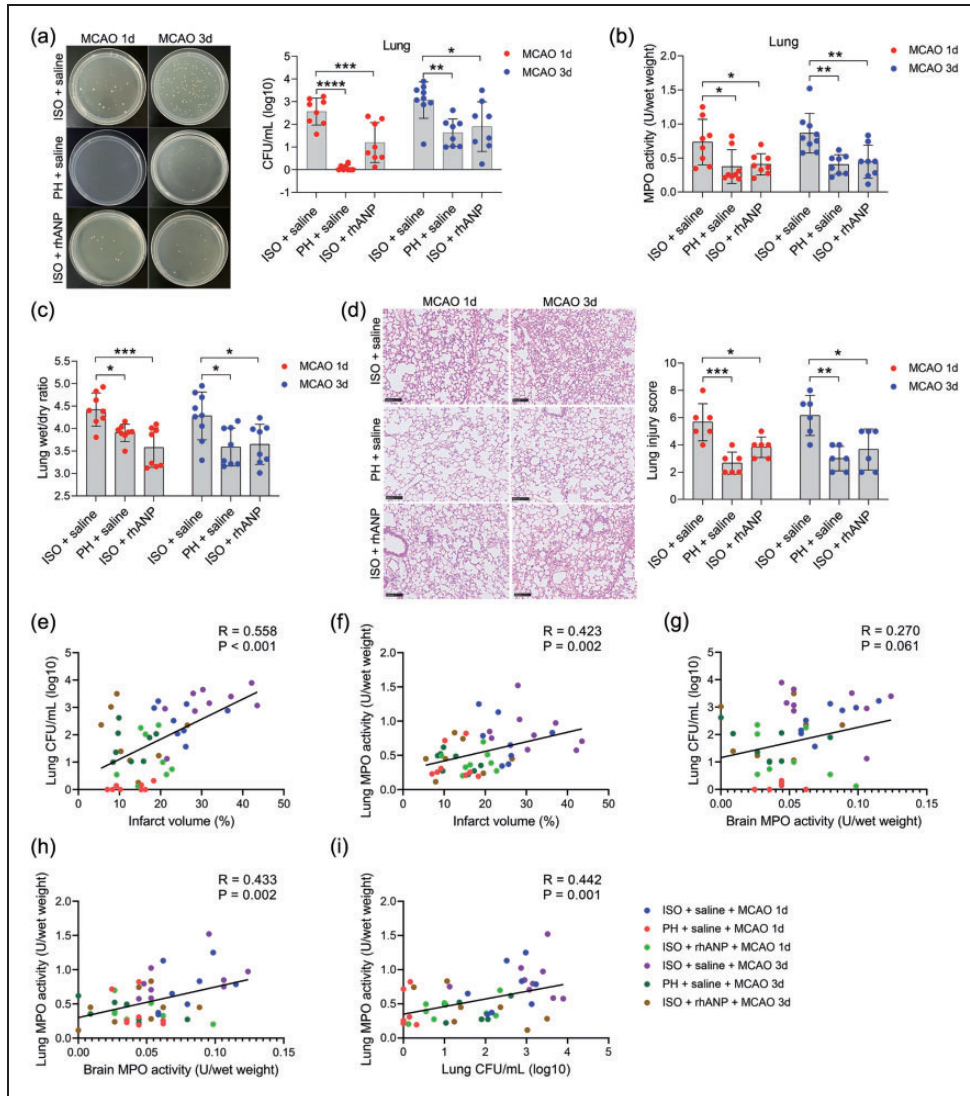


**Figure 2.** Pre-stroke ISO aggravated stroke-associated pneumonia, which could be reversed by rhANP. (a) Bacterial loads in the lungs of post-stroke mice. (b) Pulmonary MPO activity. (c) Pulmonary edema assessed by measuring the wet lung weight normalized per body weight and wet/dry lung ratio. (d) Representative H&E sections of lung and histological injury scores. Scale bar = 100  $\mu$ m. (e) Positive correlation ( $r = 0.558$ ,  $P < 0.001$ ) between brain infarct volume and the number of pulmonary CFUs. (f) Positive correlation ( $r = 0.423$ ,  $P = 0.002$ ) between brain infarct volume and pulmonary MPO activity. (g) Positive correlation ( $r = 0.27$ ,  $P = 0.061$ ) between brain infarct volume and the number of pulmonary CFUs. (h) Positive correlation ( $r = 0.433$ ,  $P = 0.002$ ) between cerebral MPO activity and pulmonary MPO activity. (i) Positive correlation ( $r = 0.558$ ,  $P < 0.001$ ) between the number of pulmonary CFUs and pulmonary MPO activity. Data are presented as individual values plus means  $\pm$  SDs ( $n = 6\text{--}9/\text{group}$ ). Comparisons were determined by one-way ANOVA followed by post hoc Newman–Keuls multiple comparison tests. Correlations were analyzed by Pearson correlation. \* $P < 0.05$ , \*\* $P < 0.01$ , \*\*\* $P < 0.001$ , \*\*\*\* $P < 0.0001$ . CFU, colony-forming units; ISO, isolated housing; MCAO, middle cerebral artery occlusion; MPO, myeloperoxidase; PH, pair housing; rhANP, recombinant human atrial natriuretic peptide.

T cells are major lymphocytes in the lamina propria and intraepithelial compartments of the small intestine, we speculated that inflammatory  $\gamma\delta$  T cells traffic into the injured brain and lung from the small intestine. We next assessed the vascular permeability of the brain, lung, jejunum and ileum. ISO mice showed striking brain and lung barrier defects relative to PH mice 24 and 72 hours after MCAO, and these defects were critically ameliorated by administering rhANP

(Figure 3(g) and (h)). Notably, coinciding with cerebral and lung barrier defects, ISO mice also exhibited elevated vascular permeability of the jejunum 24 and 72 hours following MCAO, as well as the ileum 72 hours following MCAO (Figure 3(i) and (j)). These data make it plausible that  $\gamma\delta$  T cells migrate from the intestine to the injured brain and inflamed lung during the first 3 days after MCAO, which may contribute to the progression of SAP.

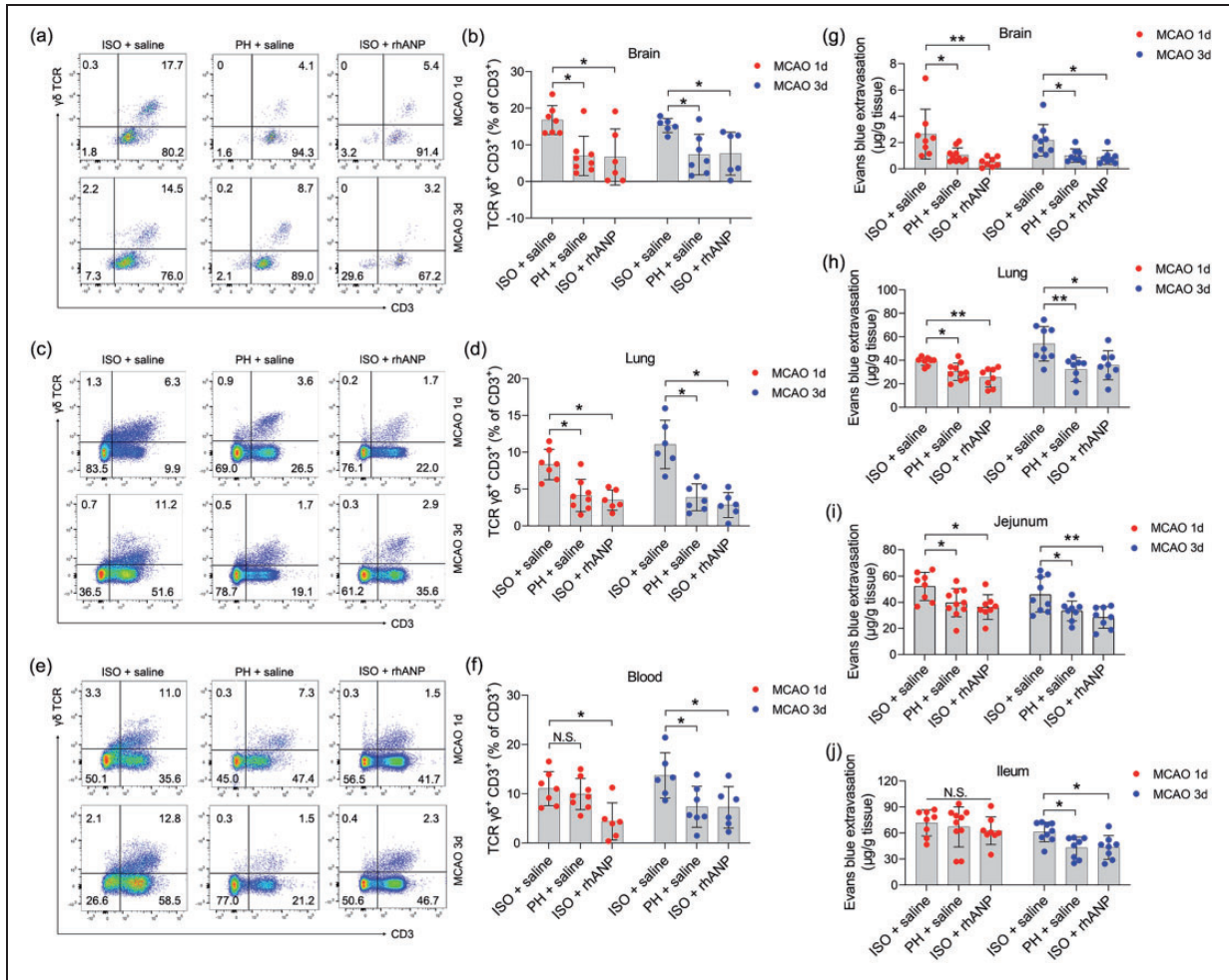


**Figure 3.** The impact of ISO and PH on the  $\gamma\delta$  T-cell levels and the vascular permeability of peripheral organs. (a, c, e) Representative flow cytometric profiles of  $\gamma\delta$  T cells ( $\text{CD3}^+ \gamma\delta \text{ TCR}^+$ ) in the brain, lung and blood of post-stroke WT mice. (b, d, f) Flow cytometry analysis of  $\gamma\delta$  T cells in the brain, lung and blood of post-stroke mice subjected to ISO or PH 24 and 72 hours after MCAO and (g–j) Determination of Evans blue extravasation in the brain, lung, jejunum and ileum in post-stroke mice. Data are presented as individual values plus means  $\pm$  SDs ( $n = 6\text{--}8/\text{group}$ ). Comparisons were determined by one-way ANOVA followed by post hoc Newman–Keuls multiple comparison tests. N.S., not significant,  $*P < 0.05$ ,  $**P < 0.01$ . ISO, isolated housing; MCAO, middle cerebral artery occlusion; PH, pair housing; rhANP, recombinant human atrial natriuretic peptide.

### Inhibitory effects of rhANP on small intestine-derived $\gamma\delta$ T-cell migration into peripheral organs after stroke

To test whether the inflammatory  $\gamma\delta$  T-cell infiltration in the brain and lung during ischemic stroke is due to direct migration of these cells from the small intestine to the injured sites, we employed Kaede-Tg mice to directly monitor cellular movements *in vivo*. All cell types of Kaede-Tg mice express the photoconvertible Kaede-Green fluorescent protein. Irradiating the small intestine with ultraviolet light can cause green fluorescence-expressing cells at the irradiated site to express red fluorescence. By examining Kaede red fluorescent protein-expressing  $\gamma\delta$  T cells in other organs, we determined the proportion of  $\gamma\delta$  T cells migrating from

the small intestine. Gating strategies of migratory  $\gamma\delta$  T cells of major organs, including that of the SI-LP, blood, brain and lung, are shown in Supplemental Figure 3, and the fluorescence conversion 24 hours post stroke can be found in Supplemental Figure 4. The migration index, which was calculated as  $\text{Kaede Red}^+ \text{CD3}^+ \gamma\delta \text{ TCR}^+ / \text{Kaede Green}^+ \text{CD3}^+$ , was used to reflect the degree of migration of  $\gamma\delta$  T cells to other sites. We found that ISO significantly enhanced the migration of  $\gamma\delta$  T cells from SI-LP compared to PH, while rhANP drastically reversed the migration-promoting effect induced by ISO (Figure 4(a) and (b)). As expected,  $\gamma\delta$  T cells of ISO mice demonstrated an increased ability to infiltrate into the brain and lung compared to that of PH mice; this increase was attenuated by rhANP treatment (Figure 4(e) to (h)).



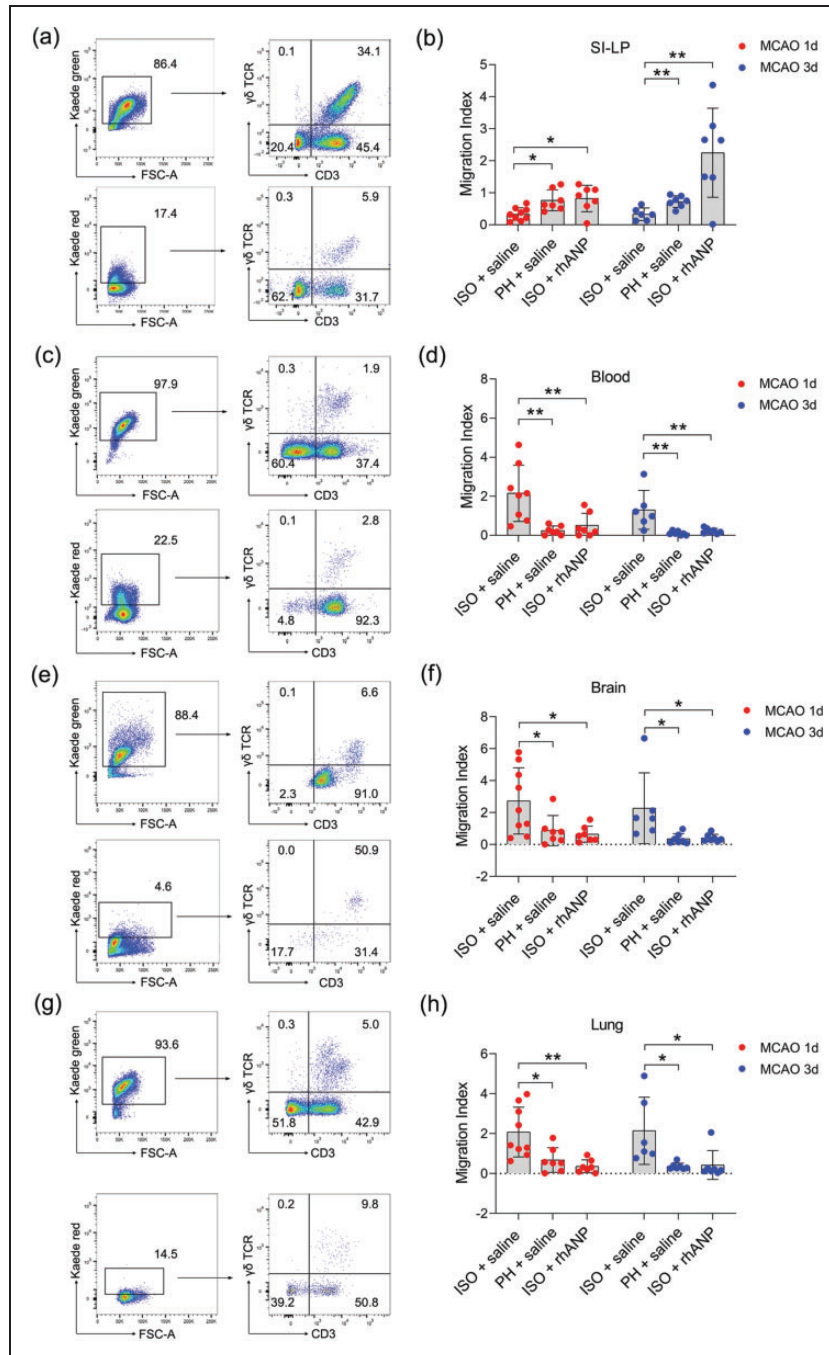


**Figure 4.** Tracking  $\gamma\delta$  T-cell migration from the small intestine to peripheral organs in Kaede-Tg mice after stroke. Representative flow cytometric plot of migratory  $\gamma\delta$  T cells of the SI-LP (a), blood (c), brain (e) and lung (g). Graph showing the extent of migration of photoconverted  $\gamma\delta$  T cells from the SI-LP (b) to blood (d), brain (f) and lung (h). The migration index was calculated as Kaede Red<sup>+</sup> CD3<sup>+</sup>  $\gamma\delta$  TCR<sup>+</sup>/Kaede Green<sup>+</sup> CD3<sup>+</sup>  $\gamma\delta$  TCR<sup>+</sup>, and represented the migration of  $\gamma\delta$  T cells to other sites. Data are presented as individual values plus means  $\pm$  SDs ( $n = 6-9$ /group). Comparisons were determined by one-way ANOVA followed by post hoc Newman-Keuls multiple comparison tests. \* $P < 0.05$ , \*\* $P < 0.01$ . ISO, isolated housing; MCAO, middle cerebral artery occlusion; PH, pair housing; rhANP, recombinant human atrial natriuretic peptide; SI-LP, lamina propria of small intestine.

Correspondingly, we also observed an analogous migratory pattern in the peripheral blood (Figure 4(c) and (d)). Interestingly,  $\gamma\delta$  T cells in ISO mice also exhibited an enhanced capacity to migrate to the liver and kidney

72 hours after MCAO (Supplemental Figure 5(b) and (c)). Moreover, rhANP treatment significantly decreased  $\gamma\delta$  T-cell migration into the liver at both 24 and 72 hours post MCAO (Supplemental Figure 5(b))



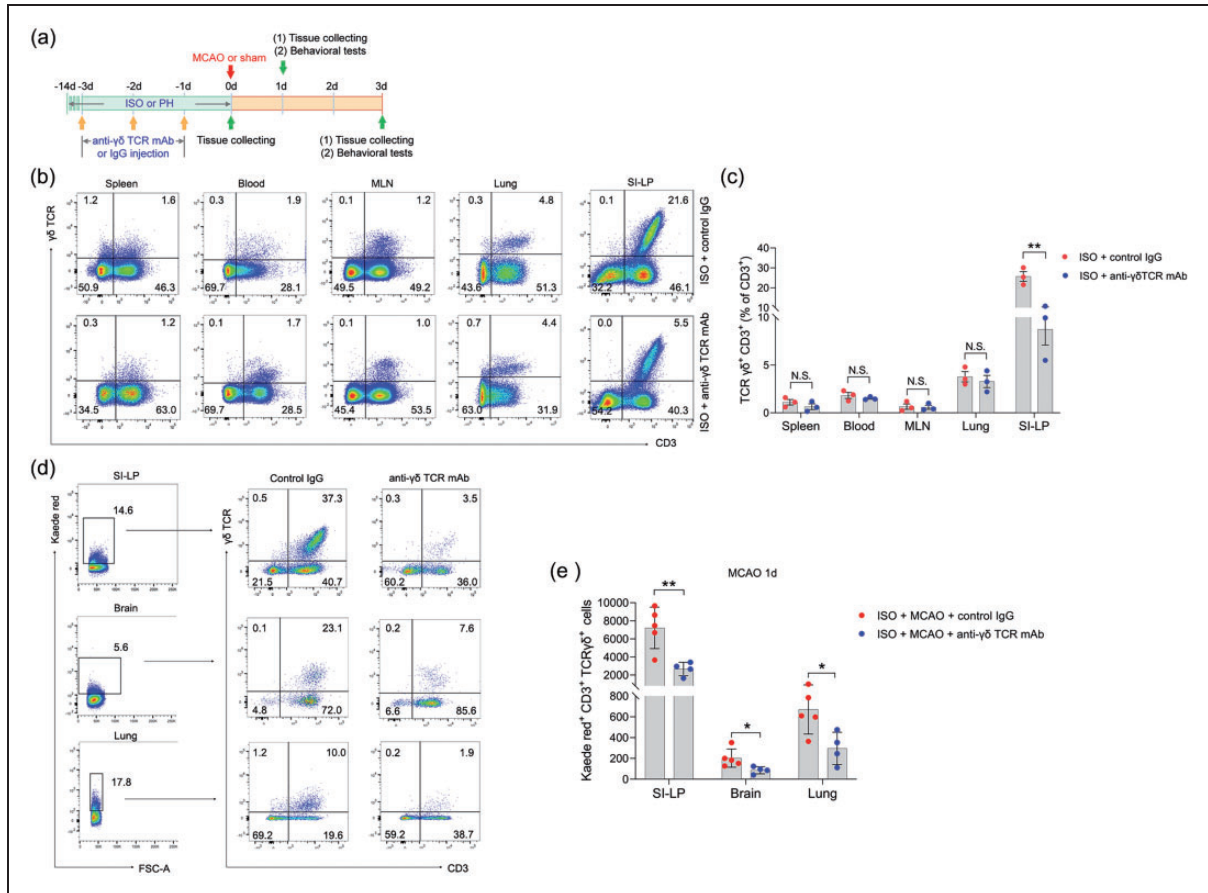


**Figure 5.** *In vivo* depleting effects of  $\gamma\delta$  TCR mAb on  $\gamma\delta$  T cells. (a) Treatment schedule. Mice were randomly assigned to ISO or PH for 14 days before MCAO or sham operation. Anti- $\gamma\delta$  TCR monoclonal antibody (500  $\mu\text{g}/\text{mouse}$  every other day for 3 days, starting 3 days before MCAO) was intravenously injected into ISO mice. PH mice and other ISO mice were sham-treated with normal hamster serum IgG. Serum, brain and lung tissues were collected on Day 1 or Day 3 post-MCAO for analysis. Behavioral tests were conducted on Day 1 or Day 3 post-MCAO. (b) Representative flow cytometric plots display the percentages of  $\gamma\delta$  T cells in the spleen, blood, lung and SI-LP. (b) The percentage of  $\gamma\delta$  T cells to total  $\text{CD3}^+$  T cells in the spleen, blood, lung and SI-LP. (d) Representative flow cytometric plots of photoconverted Kaede red  $\gamma\delta$  T cells in the SI-LP, brain and lung in post-stroke mice are shown and (e) Graph displaying the absolute numbers of Kaede red  $\gamma\delta$  T cells in the SI-LP, brain and lung. Data are presented as individual values plus means  $\pm$  SDs ( $n=3\text{--}5/\text{group}$ ). Comparisons were determined by unpaired Student's *t* test. N.S., not significant,  $*P < 0.05$ ,  $**P < 0.01$ . ISO, isolated housing; MCAO, middle cerebral artery occlusion; PH, pair housing; rhANP, recombinant human atrial natriuretic peptide; SI-LP, lamina propria of small intestine.

and into the spleen and kidney 72 hours post MCAO (Supplemental Figure 5(a) and (c)). The migration index of  $\gamma\delta$  T cells in the heart did not differ among all the groups (Supplemental Figure 5(d)).

### Protective effects of $\gamma\delta$ T-cell depletion in SAP

We then explored whether  $\gamma\delta$  T cells played an important role in ischemic stroke. To this end, we treated ISO mice with  $\gamma\delta$  TCR mAb before MCAO (Figure 5(a)). To determine the *in vivo* depleting effects of  $\gamma\delta$  TCR mAb, we analyzed the  $\gamma\delta$  T-cell levels in the spleen, blood, mesenteric lymph nodes, lung and SI-LP in ISO mice by flow cytometry at the end of the 14-day isolation period. In the SI-LP, we observed a significant reduction in  $\gamma\delta$  T cells in ISO mice subjected to  $\gamma\delta$

TCR mAb injection (Figure 5(b) and (c)). However,  $\gamma\delta$  T cells in other organs were not significantly reduced after administration of  $\gamma\delta$  TCR mAb (Figure 5(b) and (c)). We next utilized Kaede-Tg mice to further examine the depleting effect of  $\gamma\delta$  TCR mAb on  $\gamma\delta$  T cells. We noticed that ISO Kaede-Tg mice exhibited a significantly decreased number of Kaede Red<sup>+</sup>  $\gamma\delta$  T cells in the SI-LP after injection of  $\gamma\delta$  TCR mAb 24 hours post-stroke. Accordingly, Kaede Red<sup>+</sup>  $\gamma\delta$  T cells in the brain and lung also significantly declined after treatment with  $\gamma\delta$  TCR mAb (Figure 5(d) and (e)) at this time point. The data demonstrated that  $\gamma\delta$  TCR mAb treatment caused an effect only on the number of  $\gamma\delta$  T cells in the small intestine, but there was little effect on those in other organs.

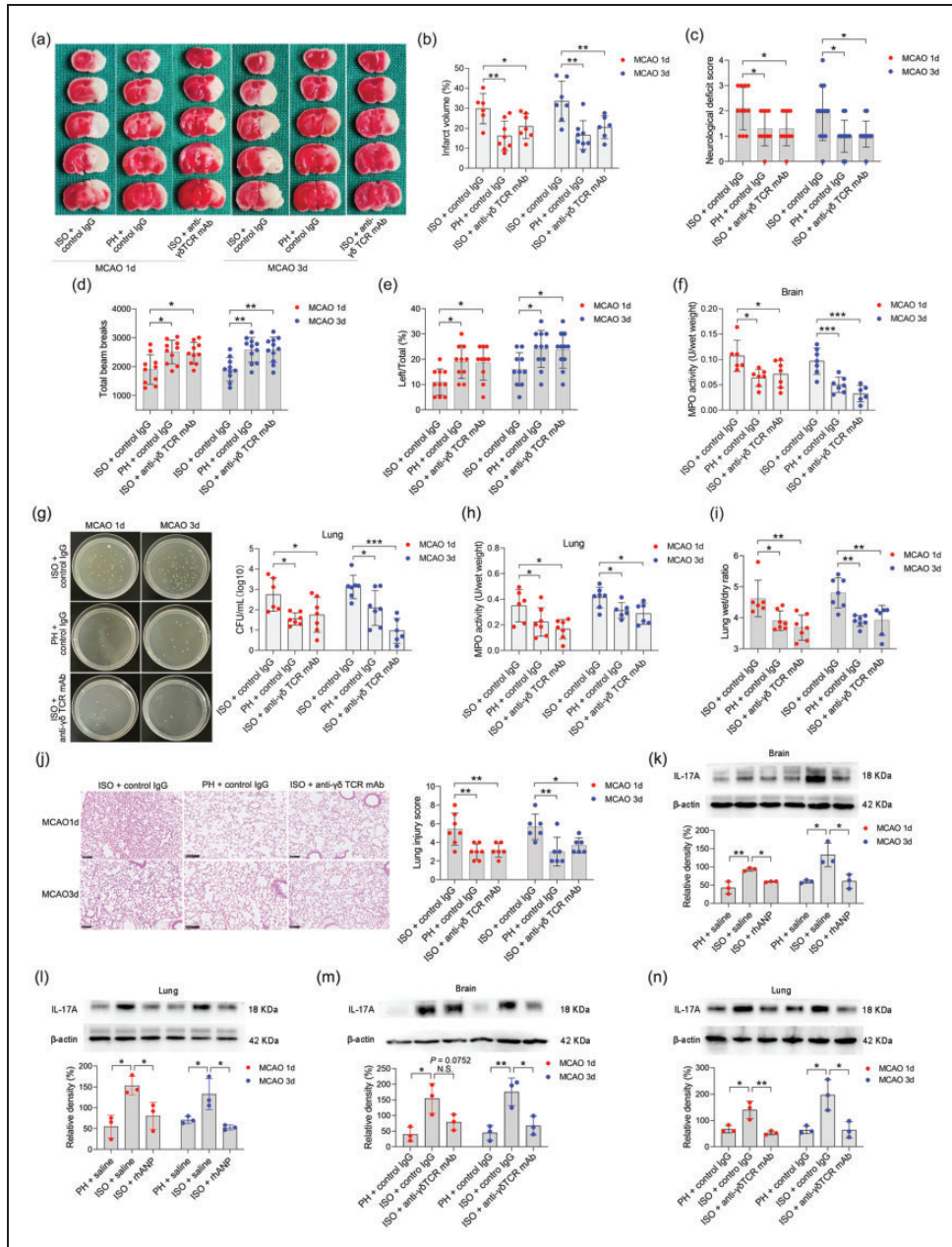


**Figure 6.**  $\gamma\delta$  T-cell depletion attenuated ISO-induced SAP exacerbation. (a, b) Infarct volumes were calculated as the percentage of infarct volume to whole brain. (c) Neurological deficit score. (d) Total beam breaks in the open field test. (e) The use of the contralateral paw in the cylinder test was determined by the percentage of left/total. (f) Cerebral MPO activity. (g) Bacterial loads in the lungs of post-stroke mice. (h) Pulmonary MPO activity. (i) Pulmonary edema assessed by measuring wet lung weight normalized per body weight and wet/dry lung ratio. (j) Representative H&E sections of lung and histological injury scores. Scale bar = 100  $\mu$ m. Western blotting analysis of IL-17A in the brain (k, m) and lung (l, n). Data are presented as individual values plus means  $\pm$  SDs ( $n = 3-12$ /group). Comparisons were determined by one-way ANOVA followed by post hoc Newman-Keuls multiple comparison tests. N.S., not significant, \* $P < 0.05$ , \*\* $P < 0.01$ , \*\*\* $P < 0.001$ . CFU, colony-forming units; ISO, isolated housing; MCAO, middle cerebral artery occlusion; MPO, myeloperoxidase; PH, pair housing; rhANP, recombinant human atrial natriuretic peptide; mAb, monoclonal antibody.

Next, we determined the potential effects of SI-LP-derived  $\gamma\delta$  T cells on neurological outcomes and bacterial pneumonia. We found that ISO mice exhibited significantly improved neurological outcomes upon anti- $\gamma\delta$  TCR mAb treatment 24 and 72 hours

after MCAO, as determined by strikingly reduced cerebral infarct volumes (Figure 6(a) and (b)), improved functional recovery (Figure 6(c) to (e)), and cerebral MPO activities (Figure 6(f)). In addition, we excluded the influence of surgical operation on the experimental

results (Supplemental Figure 1(b)). Furthermore, anti- $\gamma\delta$  TCR mAb treatment also significantly reduced the pulmonary bacterial loads and lung wet/dry weight ratio 24 and 72 hours after MCAO (Figure 6(g) to (i)). Histopathological examination of the lung tissue showed that treatment with anti- $\gamma\delta$  TCR mAb markedly reduced the tissue damage in lungs to a level that was almost comparable to that of PH mice (Figure 6(j)).

### **The role of IL-17A in $\gamma\delta$ T-cell migration-mediated SAP aggravation**

We next investigated the cellular mechanisms by which  $\gamma\delta$  T cells exert their effects. It was previously documented that  $\gamma\delta$  T cells play a potent proinflammatory role in ischemic stroke by producing various cytokines, such as IL-17A, IL-22, and IFN- $\gamma$ .<sup>48,56</sup> We then investigated the effects of anti- $\gamma\delta$  TCR mAb treatment on IL-17A, IL-22 and IFN- $\gamma$  concentrations in the brain and lung of ISO stroke mice 72 hours after stroke. We found that the levels of IL-17A in the brain and lung of ISO stroke mice significantly decreased after anti- $\gamma\delta$  T mAb intervention 72 hours after MCAO (Supplemental Figure 6(a)), but the levels of IFN- $\gamma$  and IL-22 were not significantly changed after  $\gamma\delta$  T mAb intervention (Supplementary Figure 6(b) and (c)). Meanwhile, we detected a significant decrease in the level of IL-6 after  $\gamma\delta$  T mAb treatment (Supplementary Figure 6(d)). We also observed significantly higher IL-17A expression in the brain and lung of ISO mice relative to that of PH mice 24 and 72 hours post-stroke, and this expression was inhibited by rhANP treatment (Figure 6(k) and (l)). In addition, we performed a WB assay to validate the finding that  $\gamma\delta$  T mAb treatment decreased IL-17A levels in the brains and lungs of ISO stroke mice. Our data showed that  $\gamma\delta$  TCR mAb treatment significantly reduced IL-17A expression in the brains of ISO mice 72 hours after MCAO (Figure 6(m)). IL-17A expression in the lungs of ISO mice 24 and 72 hours after MCAO was significantly decreased after anti- $\gamma\delta$  TCR mAb treatment (Figure 6(n)).

However, CD4<sup>+</sup> T helper-17 (Th17) cells are also recognized as an important cellular source of IL-17A.<sup>57</sup> However, no overt differences in Th17 cell levels were detected in the brain and blood between ISO mice, PH mice and rhANP-treated ISO mice (Supplemental Figure 7(b) and (d)). Th17 cells significantly increased in the lungs of ISO mice compared with PH mice 72 hours after MCAO (Supplemental Figure 7(a) and (c)). We then used Kaede-Tg mice to explore the migration pattern of Th17 cells in the small intestine. ISO mice has significantly more small intestine-derived Th17 cells in the lung, blood and spleen than PH mice 72 hours after MCAO (Supplemental Figure 7(g), (i) and (j)). RhANP

treatment significantly attenuated the elevation of migrated Th17 cells induced by ISO in the blood and spleen, but not in the lung 72 hours after MCAO (Supplemental Figure 7(g), (i) and (j)). Notably, ISO mice administered with rhANP exhibited significantly restrained migration of Th17 cells from the SI-LP at both 24 and 72 hours after MCAO (Supplemental Figure 7(f)). No obvious changes in Th17 cell levels in the brain and kidney were observed (Supplemental Figure 7(h) and (k)). Our data indicated that the markedly increased expression of IL-17A in the brain and lung 24 and 72 hours after MCAO was mainly derived from  $\gamma\delta$  T cells but not from CD4<sup>+</sup> Th17 cells.

### **Involvement of the subdiaphragmatic vagus nerve in mediating the migration of $\gamma\delta$ T cells**

We next sought to further explore the mechanisms by which small intestinal  $\gamma\delta$  T cells migrate into the injured brain and lung during the pathological processes of stroke. It was shown that vagus nerve signaling, an essential component of the peripheral neural network, is capable of mediating the release of lymphocytes.<sup>58</sup> We subsequently performed SDV or sham operation on Kaede-Tg mice 14 days before subjecting them to either single- or pair-housed conditions to evaluate the impact of the subdiaphragmatic vagus nerve on the migration of small intestinal  $\gamma\delta$  T cells (Figure 7(a)). In the process of establishing mouse models, cerebral blood flow during ischemia and reperfusion was measured and did not differ between treatment groups (Supplemental Figure 1(c)). We found that ISO mice that underwent SDV presented with a significantly increased number of  $\gamma\delta$  T cells in the SI-LP 72 hours post stroke (Figure 7(b) and (c)). More importantly, compared to sham surgery, SDV contributed to a marked reduction in  $\gamma\delta$  T-cell migration to the brain and lung 72 hours after MCAO (Figure 7(b) and (c)), as well as a reduction in IL-17A expression in the brain and lung of ISO mice 24 and 72 hours after MCAO (Figure 7(d) to (g)). Collectively, our data indicated that the subdiaphragmatic vagus nerve could be involved in the ISO promotion of the migration of small intestine-derived  $\gamma\delta$  T cells to inflamed loci after ischemic stroke.

## **Discussion**

In this study, we examined the effects of different pre-stroke housing conditions on brain damage and pneumonia after ischemic stroke. In contrast to social support, social isolation led to significant enlargement of cerebral infarction and more serious pneumonia. Moreover, ISO mice exhibited relatively high-grade inflammation, as indicated by elevated MPO activity



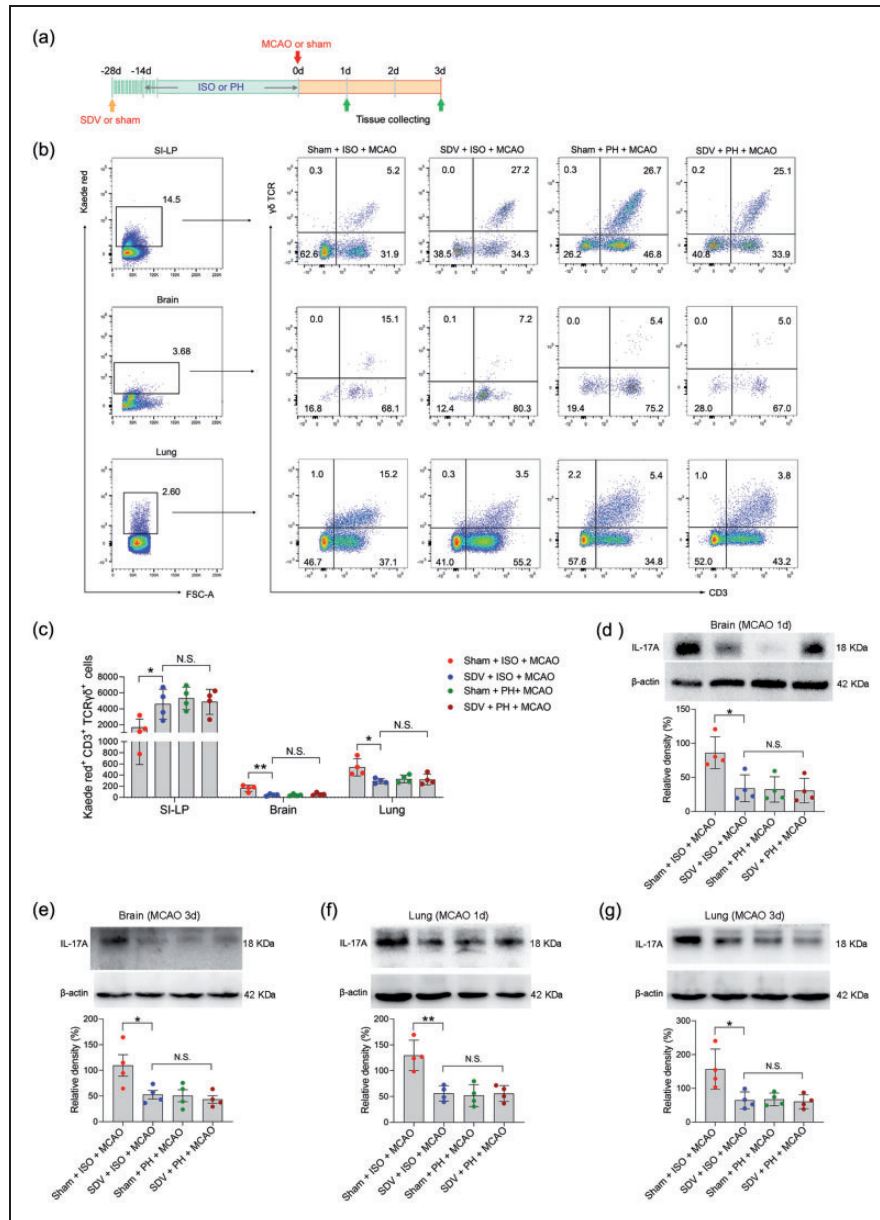


**Figure 7.** The impact of SDV on  $\gamma\delta$  T-cell migration and IL-17A expression. (a) Treatment schedule. Mice were randomly assigned to receive SDV or sham operation 28 days before MCAO or sham surgery. Fourteen days later, mice were isolated or pair-housed for 14 days. Brains and lungs were collected on Day 1 or Day 3 post-MCAO for analysis. (b) Representative flow cytometric plots of photoconverted Kaede red  $\gamma\delta$  T cells in the SI-LP, brain and lung in post-stroke mice are shown. (c) Graph displaying the absolute numbers of Kaede red<sup>+</sup>  $\gamma\delta$  T cells in the SI-LP, brain and lung. Western blotting analysis of IL-17A in the brain (d, e) and lung (f, g). Data are presented as individual values plus means  $\pm$  SDs (n = 4/group). Comparisons were determined by one-way ANOVA followed by post hoc Newman-Keuls multiple comparison tests. N.S., not significant. \* $P < 0.05$ , \*\* $P < 0.01$ . ISO, isolated housing; MCAO, middle cerebral artery occlusion; PH, pair housing; rhANP, recombinant human atrial natriuretic peptide; SDV, subdiaphragmatic vagotomy; SI-LP, lamina propria of small intestine.

and IL-17A expression in the brain and lung. Surprisingly, we found that rhANP treatment alleviated the highly inflammatory microenvironment in the brain and lung, thereby improving the prognosis after stroke. Through the exploration of cellular mechanisms, we identified  $\gamma\delta$  T cells, rather than CD4<sup>+</sup> Th17 cells, as a major source of IL-17A in the injured

brain and lung after stroke. It is worth noting that  $\gamma\delta$  T cells that migrate from the small intestine to the brain and lung have been shown to be a critical determinant of stroke exacerbation mediated by ISO. Furthermore, the subdiaphragmatic vagus nerve participated in mediating the migration of small intestine-derived  $\gamma\delta$  T cells into the brain and lung after stroke.

ISO is a stressful life event that has been linked with a higher risk for cardiovascular events and all-cause mortality.<sup>59</sup> It has been shown that more than 40% of the geriatric population suffers from poor social relationships due to social relationship alteration, including the lack of spouse company.<sup>8</sup> In particular, the number of stroke patients experiencing ISO is on the rise, particularly among elderly individuals. Emerging evidence has shown that both pre-stroke and post-stroke, ISO was highly predictive of stroke outcomes, and ISO prior to stroke was associated with 40% greater risk of adverse outcomes, including stroke recurrence and even death.<sup>12</sup> While the precise mechanisms underlying this phenomenon have yet to be clarified, it is evident that social deprivation leads to a deleterious pathological response to ischemic injury. It is widely accepted that feeling lonely or being socially isolated could overstimulate the stress response by causing the overproduction of stress hormones and the impairment of sleep quality.<sup>60</sup> In addition, preclinical experiments indicated a heightened inflammatory response in the brain and systemic circulation of ISO mice, and the elevation in systemic inflammation persists for even months after ischemic injury.<sup>15,61</sup> Conversely, experimental animals that were pair housed exhibited attenuated inflammatory responses, such as changes in the plasma concentrations of IL-6 and C-reactive protein; simultaneously, these animals had reduced infarct volume and better recovery of locomotor activity compared to socially isolated cohorts.<sup>17,62</sup> In this study, we systemically assessed the effects of pre-stroke ISO and PH on infarct volume, pneumonia, barrier dysfunction, and immune imbalance. ISO mice that underwent MCAO had worsened infarct damage and more severe pneumonia relative to paired cohorts. Importantly, we found aggravated cerebral, pulmonary and intestinal barrier damage in ISO mice. Consistent with previous research, we found that inflammatory cascades are initiated more aggressively in the brain and lung in ISO mice than in PH mice.

ANP is a 28-amino acid endocrine mediator predominantly secreted by the atrium in response to atrial stretch that is provoked by volume overload; furthermore, ANP is implicated in the modulation of body fluid homeostasis by potent diuretic, natriuretic and vasorelaxant effects.<sup>63</sup> NPRA is the predominant receptor for ANP, and NPRA is expressed on diverse organs and cells, including the lung, intestine, thymus, kidney,<sup>64–66</sup> and particularly in T lymphocytes.<sup>64,67</sup> The distribution of ANP allows it to execute its biological function in a wide range of pathophysiological processes. Evidence has shown that the plasma level of ANP is closely correlated with chronic stressors.<sup>68</sup> Research on ANP conducted in recent decades has shown that the hormone is not restricted to maintaining

volume–pressure homeostasis, but it is also essential in the modulation of cell growth and it contributes to anti-inflammatory processes.<sup>69–71</sup> Studies have shown that ANP is involved in the regulation of monocyte/macrophage functions, including phagocytosis, oxidative burst activity and inhibition of nitric oxide and tumor necrosis factor- $\alpha$  (TNF- $\alpha$ ) production.<sup>72–75</sup> ANP is also involved in stimulating the migration of human neutrophils, promoting dendritic cell-mediated Th2 cell polarization, enhancing human NK cell cytotoxicity and restraining the expression of proinflammatory mediators and adhesion molecules.<sup>21,76–79</sup> Importantly, ANP exerts barrier-protective effects by reducing LPS- and TNF- $\alpha$ -induced increases in the permeability of endothelial cells and alleviating post-septic intestinal injury.<sup>22,80</sup> Furthermore, it has been documented that exogenous ANP has a protective role in terms of both neurofunctional improvement and infarct volume reduction in experimental models of ischemic stroke.<sup>27</sup> Corroborating these findings, our study showed that exogenous administration of ANP in a dose-dependent manner decreased cerebral infarct damage and ameliorated associated pneumonia in ISO mice. It is noteworthy that administration of rhANP significantly reduced the lesion volumes in ISO stroke mice, comparable to that of PH stroke cohorts. However, in PH stroke mice, treatment with rhANP did not result in a further significant reduction in infarct volumes, possibly due to multifactorial reasons. Several factors have been demonstrated to contribute to the enlargement of infarct volumes in stroke mice, such as the joint action of a variety of immune cells and inflammatory mediators, microglial activation, and dysfunction of oxidative stress and apoptosis.<sup>81,82</sup> Although ANP plays a crucial role in stroke, its action may not counteract that of other immune factors. Therefore, simply supplementing ANP may have a limited effect on the infarct area in PH mice with small brain infarctions. Furthermore, by probing the cellular mechanisms responsible for the beneficial effects of rhANP in ischemic stroke, we found that rhANP significantly suppressed the migration of small intestine-derived  $\gamma\delta$  T cells into the brain and lung induced by pre-stroke ISO. Likewise, rhANP contributed to a marked reduction in IL-17A expression in the brain and lung of ISO mice after stroke, supporting the potent anti-inflammatory capacities of ANP. In line with our findings, Ma et al. demonstrated that ANP inhibited Th17 cell differentiation, as well as the production of IL-17A, in a dose-dependent manner.

After ischemic stroke, the blood brain barrier becomes vulnerable, allowing peripheral immune cells to infiltrate into the brain parenchyma. There is increasing evidence that the activation and infiltration of innate and adaptive immune cells into ischemic brain

regions can cause deleterious neuroinflammation after stroke.<sup>83</sup> Activated adaptive T cells invade the infarction area to exert different effects, and these cells also serve as a major inflammatory trigger for stroke progression. The activation and infiltration of CD4<sup>+</sup> and CD8<sup>+</sup> T cells exacerbate neuroinflammation and restrain the recovery from ischemic stroke.<sup>45–47</sup> The invasion of regulatory T cells has been demonstrated to play an essential role in the maintenance of brain immune homeostasis by exerting an immunosuppressive effect in the early stage of stroke.<sup>84,85</sup> The innate immune response is involved in the early phase of post-ischemic brain injury, and intrusion of peripheral innate immune cells (e.g., neutrophils, monocytes, macrophages, and natural killer cells) induces overactivation of neuroinflammation.<sup>83</sup>  $\gamma\delta$  T cells are unconventional T lymphocytes that lack MHC restriction and are considered a bridge between innate and adaptive immunity.<sup>86</sup> Although  $\gamma\delta$  T cells constitute only a minor fraction of T cells in peripheral blood, they represent the major T-cell population in mucosal and epithelial tissues, especially the gut.<sup>87</sup>  $\gamma\delta$  T cells display rapid activation and effector responses by secreting proinflammatory cytokines, including IL-17A, IL-22, IFN- $\gamma$  and TNF- $\alpha$ , which induce the recruitment of neutrophils and macrophages.<sup>88</sup> Inflammatory  $\gamma\delta$  T cells are emerging as key players in various clinical settings, including autoimmune diseases,<sup>89</sup> allergies and multiple solid tumor types in humans.<sup>44,90–92</sup> Furthermore, accumulating evidence has shown that  $\gamma\delta$  T cells not only participate in the sophisticated network in the local microenvironment of intestinal inflammation and immunity but also serve as important mediators of gut-brain axis communication.<sup>93,94</sup> We and others have demonstrated that after stroke, activation of gut inflammatory  $\gamma\delta$  T cells may drive or exacerbate ischemic brain injury by causing migration to the injury site and by producing proinflammatory cytokines (e.g., IL-17) to promote the recruitment of neutrophils and monocytes.<sup>48,49</sup> In addition, we also observed significantly higher levels of small intestine-derived  $\gamma\delta$  T cells in the inflamed lungs of ISO post-stroke mice, suggesting a critical role of  $\gamma\delta$  T cells in mediating the dysfunction of the lung-gut axis. Moreover, in murine models of psoriasis, the migration of IL-17A-producing  $\gamma\delta$  T cells between skin-draining lymph nodes and the dermis play a critical role in the pathology of psoriasis;<sup>95</sup> furthermore, depletion of  $\gamma\delta$  T cells can alleviate skin inflammation.<sup>96</sup> Collectively, these results indicate that migratory  $\gamma\delta$  T cells function as an important proinflammatory population in the induction of pathology in a variety of diseases. In our study, we observed significantly increased intestinal, cerebral and pulmonary permeability in ISO mice subjected to MCAO. The alteration

of mucosal barrier function with accompanying increased permeability has been associated with bacterial translocation and immune dysfunction and has a causal link with a variety of pathological conditions, such as inflammatory bowel disease and ischemic stroke.<sup>97–99</sup> Moreover, the intestinal inflammation promoted by elevated intestinal permeability may partly account for the transformation from protective  $\gamma\delta$  T cells to pathogenic  $\gamma\delta$  T cells.<sup>44</sup> In line with previous studies, we found that IL-17A expression was markedly elevated in the damaged lungs and brains of ISO mice after ischemic stroke, which was highly in accordance with the expression pattern of  $\gamma\delta$  T cells.  $\gamma\delta$  T cells exert a strong proinflammatory role in ischemic stroke by secreting IL-17A, IL-22, and IFN- $\gamma$ .<sup>56</sup> Our data revealed a significant decrease in IL-17A concentration in the brain and lung of ISO stroke mice, indicating the critical role of IL-17A in mediating the deleterious effect of  $\gamma\delta$  T cells in SAP. Proinflammatory IL-17A has been demonstrated to be indispensable for the recruitment of neutrophils and the exacerbation of inflammation, and although most studies have focused on IL-17A-producing CD4<sup>+</sup> T cells,  $\gamma\delta$  T cells are also a major source of IL-17A; in some autoimmune diseases, IL-17A production by  $\gamma\delta$  T cells is more pronounced than that of Th17  $\alpha\beta$  T cells.<sup>100</sup> Corroborating these findings, we found that CD4<sup>+</sup> Th17 cells did not play a primary role in the aggravation of SAP induced by ISO. Therefore, in our murine models of ischemic stroke, we postulated that IL-17A production by  $\gamma\delta$  T cells played a prominent role in the induction and promotion of deleterious inflammation and associated tissue-damaging side effects in ISO-induced SAP exacerbation. Larger infarct lesions in specific brain locations, such as the superior and lateral temporal lobe and the orbitofrontal cortex, are shown to be associated with an increased risk of SAP.<sup>101</sup> Therefore, it is noteworthy that the protective effects of pair housing on SAP, caused by inhibiting small intestine-derived  $\gamma\delta$  T-cell migration to lungs, may be directly attributable to fewer infarcts in the superior and lateral temporal lobe and the orbitofrontal cortex.

As the longest of the cranial nerves, the vagus nerve connects the brain to the peripheral organs. Information from the heart, lungs, and intestines is delivered constitutively to the brain through the vagus nerve.<sup>102</sup> Vagal signaling is now recognized as a key regulator of the communication between peripheral immune responses and the brain, with good evidence that vagotomy could attenuate the reduced social exploration induced by intraperitoneal administration of IL-1 $\beta$ .<sup>103</sup> Very recently, we revealed that SDV abrogated gut microbiota alteration-elicited neuroinflammation and cognitive dysfunction in endotoxemic mice after systemic LPS challenge.<sup>21</sup> In addition, we



have reported that SDV abrogates postseptic sleep deprivation-mediated exacerbation of systemic inflammation and multiorgan injuries.<sup>54</sup> In this study, we showed that ISO-exacerbated cerebral and pulmonary damage post-stroke may be mediated via vagal regulation of gut-derived  $\gamma\delta$  T-cell migration, as evidenced by the weakened migratory capacity of gut-derived  $\gamma\delta$  T cells to the brain and lung in mice that underwent SDV. Our results are indicative of the complexity of the bidirectional nature of vagal signaling between the periphery and brain, as well as the ability of the vagus nerve to facilitate peripheral immune signaling to the brain. Thus, recruitment of inflammatory  $\gamma\delta$  T cells into the brain might be a neuropathologic mechanism under the control of the subdiaphragmatic vagus nerve.

In conclusion, our study revealed that rhANP could alleviate ISO-aggravated ischemic cerebral damage and SAP in post-stroke mice by inhibiting small intestine-derived  $\gamma\delta$  T-cell migration to the brain and lung. The subdiaphragmatic vagus nerve mediates the migration of small intestine-derived  $\gamma\delta$  T cells into the brain and lung. However, the relationship between the subdiaphragmatic vagus nerve and ANP in alleviating pre-stroke ISO-mediated aggravation of ischemic brain injury and SAP needs to be further investigated. ANP might inhibit ISO-mediated aggravation of ischemic brain injury and SAP through subdiaphragmatic vagus nerve-mediated crosstalk between the gut and brain, as well as the lung.

### Funding

The author(s) disclosed receipt of the following financial support for the research, authorship, and/or publication of this article: This work was supported by the National Natural Science Foundation of China (82071480 [to JCZ]), the National Key Research and Development Program of China (2021YFC2501800 [to SYY]), the Japan Society for the Promotion of Science (21H00184 and 21H05612) [to KH]), and the Scientific Research Project of Hubei Provincial Health Commission (WJ2021M248 [to YY]).

### Declaration of conflicting interests

The author(s) declared no potential conflicts of interest with respect to the research, authorship, and/or publication of this article.

### Authors' contributions

JZ, YS and SY had full access to all data in the study and take responsibility for the integrity of the data and the accuracy of the data analysis. Concept and design: JZ, YS and SY. Acquisition, analysis, or interpretation of data: BX, YZ, MH, MW, YY, XC, YW. Drafting of the manuscript: BX. Critical revision of the manuscript for important intellectual content: KH. Statistical analysis: JZ and YZ. Administrative, technical, or material support: JZ, SY and YS. Supervision: JZ, YS and SY.

### Supplemental material

Supplemental material for this article is available online.

### References

1. Yu J, Wang WN, Matei N, et al. Ezetimibe attenuates oxidative stress and neuroinflammation via the AMPK/Nrf2/TXNIP pathway after MCAO in rats. *Oxid Med Cell Longev* 2020; 2020: 1–14.
2. Eltringham SA, Smith CJ, Pownall S, et al. Variation in dysphagia assessment and management in acute stroke: an interview study. *Geriatrics (Basel)* 2019; 4: 60.
3. Ge H, Zhang C, Yang Y, et al. Ambroxol upregulates glucocerebrosidase expression to promote neural stem cells differentiation into neurons through wnt/ $\beta$ -catenin pathway after ischemic stroke. *Front Mol Neurosci* 2020; 13: 596039.
4. Jin R, Liu S, Wang M, et al. Inhibition of CD147 attenuates Stroke-Associated pneumonia through modulating lung immune response in mice. *Front Neurol* 2019; 10: 853.
5. Farris BY, Monaghan KL, Zheng W, et al. Ischemic stroke alters immune cell niche and chemokine profile in mice independent of spontaneous bacterial infection. *Immun Inflamm Dis* 2019; 7: 326–341.
6. Kalra L, Irshad S, Hodsoll J, et al. Prophylactic antibiotics after acute stroke for reducing pneumonia in patients with dysphagia (stroke-inf): a prospective, cluster-randomised, open-label, masked endpoint, controlled clinical trial. *Lancet* 2015; 386: 1835–1844.
7. Meisel A and Smith CJ. Prevention of stroke-associated pneumonia: where next? *Lancet* 2015; 386: 1802–1804.
8. Cudjoe T, Roth DL, Szanton SL, et al. The epidemiology of social isolation: national health and aging trends study. *J Gerontol B Psychol Sci Soc Sci* 2020; 75: 107–113.
9. Zhou Z, Lin C, Ma J, et al. The association of social isolation with the risk of stroke among middle-aged and older adults in China. *Am J Epidemiol* 2019; 188: 1456–1465.
10. Valtorta NK, Kanaan M, Gilbody S, et al. Loneliness and social isolation as risk factors for coronary heart disease and stroke: systematic review and meta-analysis of longitudinal observational studies. *Heart* 2016; 102: 1009–1016.
11. Liu X, Yu HJ, Gao Y, et al. Combined association of multiple chronic diseases and social isolation with the functional disability after stroke in elderly patients: a multicenter cross-sectional study in China. *BMC Geriatr* 2021; 21: 495.
12. Boden-Albala B, Litwak E, Elkind MS, et al. Social isolation and outcomes post stroke. *Neurology* 2005; 64: 1888–1892.
13. Saadi A, Okeng'O K, Biseko MR, et al. Post-stroke social networks, depressive symptoms, and disability in Tanzania: a prospective study. *Int J Stroke* 2018; 13: 840–848.
14. Holmes A, Xu Y, Lee J, et al. Post-stroke social isolation reduces cell proliferation in the dentate gyrus and

- alters miRNA profiles in the aged female mice brain. *IJMS* 2020; 22: 99.
15. Verma R, Harris NM, Friedler BD, et al. Reversal of the detrimental effects of post-stroke social isolation by pair-housing is mediated by activation of BDNF-MAPK/ERK in aged mice. *Sci Rep* 2016; 6: 25176.
  16. Verma R, Friedler BD, Harris NM, et al. Pair housing reverses post-stroke depressive behavior in mice. *Behav Brain Res* 2014; 269: 155–163.
  17. Craft TK, Gasper ER, McCullough L, et al. Social interaction improves experimental stroke outcome. *Stroke* 2005; 36: 2006–2011.
  18. Nakagawa Y, Nishikimi T and Kuwahara K. Atrial and brain natriuretic peptides: hormones secreted from the heart. *Peptides* 2019; 111: 18–25.
  19. De Vito P. Atrial natriuretic peptide: an old hormone or a new cytokine? *Peptides* 2014; 58: 108–116.
  20. Kitakaze M, Asakura M, Kim J, et al. Human atrial natriuretic peptide and nicorandil as adjuncts to reperfusion treatment for acute myocardial infarction (J-WIND): two randomised trials. *Lancet* 2007; 370: 1483–1493.
  21. Wu Y, Zhang Y, Xie B, et al. RhANP attenuates endotoxin-derived cognitive dysfunction through subdiaphragmatic vagus nerve-mediated gut microbiota-brain axis. *J Neuroinflammation* 2021; 18: 300.
  22. Xing J and Birukova AA. ANP attenuates inflammatory signaling and rho pathway of lung endothelial permeability induced by LPS and TNFalpha. *Microvasc Res* 2010; 79: 56–62.
  23. Zhu YB, Zhang YB, Liu DH, et al. Atrial natriuretic peptide attenuates inflammatory responses on oleic acid-induced acute lung injury model in rats. *Chin Med J (Engl)* 2013; 126: 747–750.
  24. Zhang Y, Xie B, Yuan Y, et al. (R,S)-ketamine promotes striatal neurogenesis and sensorimotor recovery through improving poststroke depression-mediated decrease in atrial natriuretic peptide. *Biol Psychiatry Glob Open Sci* 2021; 1: 90–100.
  25. Bandelow B, Baldwin D, Abelli M, et al. Biological markers for anxiety disorders, OCD and PTSD: a consensus statement. Part II: neurochemistry, neurophysiology and neurocognition. *World J Biol Psychiatry* 2017; 18: 162–214.
  26. Wisen AG, Ekberg K, Wohlfart B, et al. Plasma ANP and BNP during exercise in patients with major depressive disorder and in healthy controls. *J Affect Disord* 2011; 129: 371–375.
  27. Lopez-Morales MA, Castello-Ruiz M, Burguete MC, et al. Molecular mechanisms underlying the neuroprotective role of atrial natriuretic peptide in experimental acute ischemic stroke. *Mol Cell Endocrinol* 2018; 472: 1–9.
  28. Pereira NL, Tosakulwong N, Scott CG, et al. Circulating atrial natriuretic peptide genetic association study identifies a novel gene cluster associated with stroke in whites. *Circ Cardiovasc Genet* 2015; 8: 141–149.
  29. Nogami M, Shiga J, Takatsu A, et al. Immunohistochemistry of atrial natriuretic peptide in brain infarction. *Histochem J* 2001; 33: 87–90.
  30. Tsukagoshi H, Shimizu Y, Kawata T, et al. Atrial natriuretic peptide inhibits tumor necrosis factor-alpha production by interferon-gamma-activated macrophages via suppression of p38 mitogen-activated protein kinase and nuclear factor-kappa B activation. *Regul Pept* 2001; 99: 21–29.
  31. Chen C, Zhang Y, Tao M, et al. Atrial natriuretic peptide attenuates colitis via inhibition of the cGAS-STING pathway in colonic epithelial cells. *Int J Biol Sci* 2022; 18: 1737–1754.
  32. Han L, Wang XM, Di S, et al. Innate lymphoid cells: a link between the nervous system and microbiota in intestinal networks. *Mediators Inflamm* 2019; 2019: 1–11.
  33. Hattori N and Yamashiro Y. The gut-brain axis. *Ann Nutr Metab* 2021; 77 Suppl: 1–3.
  34. Zhang J, Ma L, Chang L, et al. A key role of the subdiaphragmatic vagus nerve in the depression-like phenotype and abnormal composition of gut microbiota in mice after lipopolysaccharide administration. *Transl Psychiatry* 2020; 10: 186.
  35. Dickson RP, Singer BH, Newstead MW, et al. Enrichment of the lung microbiome with gut bacteria in sepsis and the acute respiratory distress syndrome. *Nat Microbiol* 2016; 1: 16113.
  36. Dessein R, Bauduin M, Grandjean T, et al. Antibiotic-related gut dysbiosis induces lung immunodepression and worsens lung infection in mice. *Crit Care* 2020; 24: 611.
  37. Wang Z, Bai C, Hu T, et al. Emerging trends and hotspot in gut-lung axis research from 2011 to 2021: a bibliometrics analysis. *Biomed Eng Online* 2022; 21: 27.
  38. Tripathi A, Debelius J, Brenner DA, et al. The gut-liver axis and the intersection with the microbiome. *Nat Rev Gastroenterol Hepatol* 2018; 15: 397–411.
  39. Arya AK and Hu B. Brain-gut axis after stroke. *Brain Circ* 2018; 4: 165–173.
  40. Honarpisheh P, Bryan RM and McCullough LD. Aging microbiota-gut-brain axis in stroke risk and outcome. *Circ Res* 2022; 130: 1112–1144.
  41. Jagdmann S, Berchtold D, Gutbier B, et al. Efficacy and safety of intratracheal IFN- $\gamma$  treatment to reverse stroke-induced susceptibility to pulmonary bacterial infections. *J Neuroimmunol* 2021; 355: 577568.
  42. Nielsen MM, Witherden DA and Havran WL.  $\gamma\delta$  T cells in homeostasis and host defence of epithelial barrier tissues. *Nat Rev Immunol* 2017; 17: 733–745.
  43. Lu H, Li DJ and Jin LP.  $\gamma\delta$ T cells and related diseases. *Am J Reprod Immunol* 2016; 75: 609–618.
  44. Wu P, Wu D, Ni C, et al.  $\gamma\delta$ T17 cells promote the accumulation and expansion of myeloid-derived suppressor cells in human colorectal cancer. *Immunity* 2014; 40: 785–800.
  45. Shaw BC, Maglinger GB, Ujas T, et al. Isolation and identification of leukocyte populations in intracranial blood collected during mechanical thrombectomy. *J Cereb Blood Flow Metab* 2022; 42: 280–291.
  46. Brown J, Kingsbury C, Lee J-Y, et al. Spleen participation in partial MHC class II construct neuroprotection in stroke. *CNS Neurosci Ther* 2020; 26: 663–669.

47. Zhou YX and Wang X. 2mAb reduces demyelination after focal cerebral ischemia by suppressing CD8<sup>+</sup> T cells. *CNS Neurosci Ther* 2019; 25: 532–543.
48. Shichita T, Sugiyama Y, Ooboshi H, et al. Pivotal role of cerebral interleukin-17-producing gammadelta T cells in the delayed phase of ischemic brain injury. *Nat Med* 2009; 15: 946–950.
49. Gelderblom M, Weymar A, Bernreuther C, et al. Neutralization of the IL-17 axis diminishes neutrophil invasion and protects from ischemic stroke. *Blood* 2012; 120: 3793–3802.
50. Zhang Y, Xu D, Qi H, et al. Enriched environment promotes post-stroke neurogenesis through NF- $\kappa$ B-mediated secretion of IL-17A from astrocytes. *Brain Res* 2018; 1687: 20–31.
51. Yao H, Zhang Y, Shu H, et al. Hyperforin promotes post-stroke neuroangiogenesis via astrocytic IL-6-mediated negative immune regulation in the ischemic brain. *Front Cell Neurosci* 2019; 13: 201.
52. Zhang Y, Yu P, Liu H, et al. Hyperforin improves post-stroke social isolation-induced exaggeration of PSD and PSA via TGF- $\beta$ . *Int J Mol Med* 2019; 43: 413–425.
53. Lin Y, Zhang JC, Yao CY, et al. Critical role of astrocytic interleukin-17 a in post-stroke survival and neuronal differentiation of neural precursor cells in adult mice. *Cell Death Dis* 2016; 7: e2273–e2273.
54. Zhang Y, Xie B, Chen X, et al. A key role of gut microbiota-vagus nerve/spleen axis in sleep deprivation-mediated aggravation of systemic inflammation after LPS administration. *Life Sci* 2021; 265: 118736.
55. Xie B, Zhang Y, Qi H, et al. Red light exaggerated sepsis-induced learning impairments and anxiety-like behaviors. *Aging (Albany NY)* 2020; 12: 23739–23760.
56. Wang L, Yao C, Chen J, et al.  $\gamma\delta$  T cell in cerebral ischemic stroke: characteristic, immunity-inflammatory role, and therapy. *Front Neurol* 2022; 13: 842212.
57. Jiang P, Zheng C, Xiang Y, et al. The involvement of TH17 cells in the pathogenesis of IBD. *Cytokine Growth Factor Rev* 2022; S1359-6101: 00053–00053.
58. Antonica A, Magni F, Mearini L, et al. Vagal control of lymphocyte release from rat thymus. *J Auton Nerv Syst* 1994; 48: 187–197.
59. Holt-Lunstad J, Smith TB and Layton JB. Social relationships and mortality risk: a meta-analytic review. *Plos Med* 2010; 7: e1000316.
60. Cacioppo S, Capitanio JP and Cacioppo JT. Toward a neurology of loneliness. *Psychol Bull* 2014; 140: 1464–1504.
61. Caso JR, Moro MA, Lorenzo P, et al. Involvement of IL-1beta in acute stress-induced worsening of cerebral ischaemia in rats. *Eur Neuropsychopharmacol* 2007; 17: 600–607.
62. Karelina K, Norman GJ, Zhang N, et al. Social contact influences histological and behavioral outcomes following cerebral ischemia. *Exp Neurol* 2009; 220: 276–282.
63. Gruden G, Landi A and Bruno G. Natriuretic peptides, heart, and adipose tissue: new findings and future developments for diabetes research. *Diabetes Care* 2014; 37: 2899–2908.
64. Misono KS. Natriuretic peptide receptor: structure and signaling. *Mol Cell Biochem* 2002; 230: 49–60.
65. Potter LR, Yoder AR and Flora DR. Natriuretic peptides: their structures, receptors, physiologic functions and therapeutic applications. *Handb Exp Pharmacol* 2009; 191: 341–366.
66. Tallerico-Melnyk T, Yip CC and Watt VM. Widespread co-localization of mRNAs encoding the guanylate cyclase-coupled natriuretic peptide receptors in rat tissues. *Biochem Biophys Res Commun* 1992; 189: 610–616.
67. Mohapatra SS, Lockey RF, Vesely DL, et al. Natriuretic peptides and genesis of asthma: an emerging paradigm? *J Allergy Clin Immunol* 2004; 114: 520–526.
68. Wann BP, Audet MC, Gibb J, et al. Anhedonia and altered cardiac atrial natriuretic peptide following chronic stressor and endotoxin treatment in mice. *Psychoneuroendocrinology* 2010; 35: 233–240.
69. Ma L, Li J, Wang G, et al. Atrial natriuretic peptide suppresses Th17 development through regulation of cGMP-dependent protein kinase and PI3K-Akt signaling pathways. *Regul Pept* 2013; 181: 9–16.
70. De Vito P, Incerpi S, Pedersen JZ, et al. Atrial natriuretic peptide and oxidative stress. *Peptides* 2010; 31: 1412–1419.
71. De Vito P, Incerpi S, Affabris E, et al. Effect of atrial natriuretic peptide on reactive oxygen species-induced by hydrogen peroxide in thp-1 monocytes: role in cell growth, migration and cytokine release. *Peptides* 2013; 50: 100–108.
72. Kierner AK and Vollmar AM. Autocrine regulation of inducible nitric-oxide synthase in macrophages by atrial natriuretic peptide. *J Biol Chem* 1998; 273: 13444–13451.
73. Kierner AK and Vollmar AM. The atrial natriuretic peptide regulates the production of inflammatory mediators in macrophages. *Ann Rheum Dis* 2001; 60 Suppl 3: iii68–70.
74. Vollmar AM, Forster R and Schulz R. Effects of atrial natriuretic peptide on phagocytosis and respiratory burst in murine macrophages. *Eur J Pharmacol* 1997; 319: 279–285.
75. Kierner AK, Hartung T and Vollmar AM. cGMP-mediated inhibition of TNF-alpha production by the atrial natriuretic peptide in murine macrophages. *J Immunol* 2000; 165: 175–181.
76. Weber NC, Blumenthal SB, Hartung T, et al. ANP inhibits TNF-alpha-induced endothelial MCP-1 expression—involvement of p38 MAPK and MKP-1. *J Leukoc Biol* 2003; 74: 932–941.
77. Izumi T, Saito Y, Kishimoto I, et al. Blockade of the natriuretic peptide receptor guanylyl cyclase-A inhibits NF-kappaB activation and alleviates myocardial ischemia/reperfusion injury. *J Clin Invest* 2001; 108: 203–213.
78. Morita R, Ukyo N, Furuya M, et al. Atrial natriuretic peptide polarizes human dendritic cells toward a Th2-promoting phenotype through its receptor guanylyl cyclase-coupled receptor A. *J Immunol* 2003; 170: 5869–5875.



79. Moss RB and Golightly MG. In vitro enhancement of natural cytotoxicity by atrial natriuretic peptide fragment 4-28. *Peptides* 1991; 12: 851–854.
80. Elbaradey GF, Elshmaa NS and Hodeib H. The effect of atrial natriuretic peptide infusion on intestinal injury in septic shock. *J Anaesthesiol Clin Pharmacol* 2016; 32: 470–475.
81. Zhai LP, Pei HY, Shen HP, et al. Mechanism of neocryptotanshinone in protecting against cerebral ischemic injury: by suppressing M1 Polarization of microglial cells and promoting cerebral angiogenesis. *Int Immunopharmacol* 2023; 116: 109815.
82. Zheng HW, Guo X, Kang SM, et al. Cdh5-mediated Fpn1 deletion exerts neuroprotective effects during the acute phase and inhibitory effects during the recovery phase of ischemic stroke. *Cell Death Dis* 2023; 14: 161.
83. Xie L, Li W, Hersh J, et al. Experimental ischemic stroke induces long-term T cell activation in the brain. *J Cereb Blood Flow Metab* 2019; 39: 2268–2276.
84. Xie W and Li P. Visualizing regulatory lymphocytic responses to predict neurological outcome after stroke. *Cns Neurosci Ther* 2021; 27: 867–868.
85. Wang H, Wang Z, Wu Q, et al. Regulatory T cells in ischemic stroke. *Cns Neurosci Ther* 2021; 27: 643–651.
86. Godfrey DI, Uldrich AP, McCluskey J, et al. The burgeoning family of unconventional T cells. *Nat Immunol* 2015; 16: 1114–1123.
87. Mowat AM and Agace WW. Regional specialization within the intestinal immune system. *Nat Rev Immunol* 2014; 14: 667–685.
88. Vantourout P and Hayday A. Six-of-the-best: unique contributions of  $\gamma\delta$  T cells to immunology. *Nat Rev Immunol* 2013; 13: 88–100.
89. Zarobkiewicz MK, Kowalska W, Roliński J, et al.  $\gamma\delta$  T lymphocytes in the pathogenesis of multiple sclerosis and experimental autoimmune encephalomyelitis. *J Neuroimmunol* 2019; 330: 67–73.
90. Daley D, Zambirinis CP, Seifert L, et al.  $\gamma\delta$  T cells support pancreatic oncogenesis by restraining  $\alpha\beta$  T cell activation. *Cell* 2016; 166: 1485–1499.e15.
91. Castillo-González R, Cibrian D and Sánchez-Madrid F. Dissecting the complexity of  $\gamma\delta$  T-cell subsets in skin homeostasis, inflammation, and malignancy. *J Allergy Clin Immunol* 2021; 147: 2030–2042.
92. Silva-Santos B, Serre K and Norell H.  $\gamma\delta$  T cells in cancer. *Nat Rev Immunol* 2015; 15: 683–691.
93. Albertsson AM, Zhang X, Vontell R, et al.  $\gamma\delta$  T cells contribute to injury in the developing brain. *Am J Pathol* 2018; 188: 757–767.
94. Seki D, Mayer M, Hausmann B, et al. Aberrant gut-microbiota-immune-brain axis development in premature neonates with brain damage. *Cell Host Microbe* 2021; 29: 1558–1572.e6.
95. Ramirez-Valle F, Gray EE and Cyster JG. Inflammation induces dermal  $V\gamma 4^+$   $\gamma\delta$ T17 memory-like cells that travel to distant skin and accelerate secondary IL-17-driven responses. *Proc Natl Acad Sci U S A* 2015; 112: 8046–8051.
96. Li M, Cheng H, Tian D, et al. D-Mannose suppresses  $\gamma\delta$  T cells and alleviates murine psoriasis. *Front Immunol* 2022; 13: 840755.
97. Stanley D, Mason LJ, Mackin KE, et al. Translocation and dissemination of commensal bacteria in post-stroke infection. *Nat Med* 2016; 22: 1277–1284.
98. Sanchez DMF, Romero-Calvo I, Mascaraque C, et al. Intestinal inflammation and mucosal barrier function. *Inflamm Bowel Dis* 2014; 20: 2394–2404.
99. Benakis C, Brea D, Caballero S, et al. Commensal microbiota affects ischemic stroke outcome by regulating intestinal  $\gamma\delta$  T cells. *Nat Med* 2016; 22: 516–523.
100. Ma Y, Aymeric L, Locher C, et al. Contribution of IL-17-producing gamma delta T cells to the efficacy of anti-cancer chemotherapy. *J Exp Med* 2011; 208: 491–503.
101. Urra X, Laredo C, Zhao Y, et al. Neuroanatomical correlates of stroke-associated infection and stroke-induced immunodepression. *Brain Behav Immun* 2017; 60: 142–150.
102. Forsythe P, Bienenstock J and Kunze WA. Vagal pathways for microbiome-brain-gut axis communication. *Adv Exp Med Biol* 2014; 817: 115–133.
103. Luheshi GN, Bluthé RM, Rushforth D, et al. Vagotomy attenuates the behavioural but not the pyrogenic effects of interleukin-1 in rats. *Auton Neurosci* 2000; 85: 127–132.